



Published in final edited form as:

*Appl Spectrosc.* 2011 April ; 65(4): 115–124. doi:10.1366/10-06224.

## Fluorescence Correlation Spectroscopy: A Review of Biochemical and Microfluidic Applications

Yu Tian, Michelle M. Martinez, and Dimitri Pappas

Department of Chemistry and Biochemistry, Texas Tech University, Lubbock, TX 79409

Dimitri Pappas: d.pappas@ttu.edu

### Abstract

Over the years fluorescence correlation spectroscopy (FCS) has proven to be a useful technique that has been utilized in several fields of study. Although FCS initially suffered from poor signal to noise ratios, the incorporation of confocal microscopy has overcome this drawback and transformed FCS into a sensitive technique with high figures of merit. In addition, tandem methods have evolved to include dual-color cross-correlation, total internal reflection fluorescence correlation, and fluorescence lifetime correlation spectroscopy combined with time-correlated single photon counting. In this review, we discuss several applications of FCS for biochemical, microfluidic, and cellular investigations.

### Introduction

Fluorescence correlation spectroscopy (FCS) was first introduced as an analytical method applied for chemical dynamics of DNA-drug intercalation by Magde, Elson and Webb in the early 1970s.<sup>1–3</sup> However, due to poor signal-to-noise ratios this technique did not become extensively used until FCS was combined with confocal detection, which could overcome low detection efficiency, large molecule numbers and insufficient suppression of background fluorescence and scattered light.<sup>4</sup> To date, in view of the advantages of high spatial and temporal resolution, short analysis time, and little sample consumption<sup>5,6</sup>, FCS has gradually developed as a method for the study of chemical kinetics, conformation dynamics, and molecular diffusion in solution and on membranes.<sup>2,7,8</sup> In most fluorescence techniques, the intensity of the fluorescence signal is the measured parameter. For example, in fluorescence lifetime, the decay of fluorescence is measured, whereas in fluorescence anisotropy the polarized components of the emission are detected. In FCS, the parameter of interest is the fluctuation of the fluorescence intensity. This fluctuation occurs from random effects (noise) as well as chemical, biological, and physical effects on the fluorophore of interest. These slight fluctuations serve as a carrier wave of information and are, in essence, decoded during the correlation measurement to yield meaningful data about the environment in which a fluorophore resides. Chemical changes include equilibria, reactions, complexation, quenching, etc. Physical changes include molecular motion, photophysical interactions, and changes in conformation can also affect fluorescence emission. From a biological standpoint, anomalous diffusion, association of molecules into complex superstructures, and other aggregation phenomena also affect the fluorescence fluctuations. FCS can therefore be used to investigate these and other chemical, physical, and biological phenomena, provided an accurate fluorescence model can be derived. FCS also possess a large temporal linear dynamic range, from nanoseconds to minutes, in a single measurement.

One of the key breakthroughs in FCS has been the improvements in microscope design and detector efficiency, allowing single-molecule sensitivity to be coupled to FCS. Advances in instrument design and optical approaches have allowed FCS to be applied to increasingly complex problems that cannot be solved by other methods. One of the key advantages of FCS is that it is an *in situ*, nondestructive and largely non-perturbing technique. As a result, FCS has gained significant acceptance in the fields of biology and microfluidics. In both cases, complex systems need to be assayed with minimal perturbation. At the same time, fluorescence techniques have been associated with biochemical and microfluidic analyses.

FCS has become an established tool for concentration and aggregation measurements, diffusion analysis and molecular interaction determination.<sup>9–15</sup> Recently, FCS has also been employed to investigate the molecular motion and receptor density on live cells and tissues.<sup>16</sup> For example, subdiffusive motion was studied in nanochannels by FCS, and the influence of confinements on different molecule motions was investigated.<sup>17</sup> Besides the study of diffusion-based transport without flow, FCS can be applied to profile the flow through confocal detection. GÖsch has first reported using FCS to determine two-dimensional laminar flow profiles in a Y-shape microchannel.<sup>5</sup> Liu and co-workers featured the fluidic vortex generating at a T-shape junction across a microfluidic channel using FCS.<sup>18</sup> The Visser group investigated flowing fluorescent particles in a microcapillary to determine the flow velocity and study optical forces produced by laser beam.<sup>6</sup> Researchers at Cornell University characterized the hydrodynamic properties of a five-inlet port microfluidic mixer which was designed for the investigations of kinetic reactions of macromolecules and monitored diffusive mixing using FCS.<sup>19</sup> In these example papers, FCS has proven to be a powerful technique for the studies of fluidic characterization either in microchannels or capillaries.

Although FCS has been applied to monitor many chemical and biochemical processes, this technique still has some limitations of misleading calculations under different environments and the lack of interpreting models.<sup>20–23</sup> To overcome these artifacts, novel techniques have been developed as extensions of FCS, and are more widely used in flow measurement and investigation of molecular diffusion in membrane. Fluorescence cross-correlation spectroscopy (FCCS) has been applied to study the dynamics and interactions of molecules. Recently, Lee and co-workers developed an instrument for cross-talk-free FCCS, which has been employed to study the enzymatic activity in their work.<sup>24</sup> In the Burden group, numerical fluorescence correlation spectroscopy (NFCS), which circumvented many limitations of traditional FCS, was used to measure diffusion even when there were special aberrations in the probe volume.<sup>25</sup> Arbour reported that due to dual-focus modifications and external length scale hallmark, dual-focus FCS was more reliable and useful when it was used for measuring flow profiles in microfluidic channels.<sup>26</sup> Diffusion measurement in lipid bilayers could suffer from the slow motion which can lead to photobleaching and instabilities of in sample. Scanning FCS has been developed and solved this problem by reducing the exposure time of moving fluorophores to the excitation laser beam.<sup>27–29</sup>

In addition to correlation and cross-correlation measurements, fluorescence lifetime correlation spectroscopy (FLCS) combined FCS with Time-Correlated Single Photon Counting (TCSPC), which makes it possible to recognize the contribution of fluorophores in a mixture system.<sup>30</sup> Wennmalm reported using inverse- Fluorescence correlation spectroscopy (iFCS) to analyze particle size and concentrations of unlabeled molecules based on the principle that signals come from medium surrounding interested particles but not from particles themselves.<sup>31</sup>

These aforementioned examples are but a small group of applications of FCS and its related techniques. FCS has proven to be a powerful probe into dynamic systems, and will continue

to gain in popularity due to its sensitivity to the probed environment. New approaches to measurement fluorescence correlation and cross-correlation have resulted in better interpretive models, more accurate data, and simplified operation. These extensions of FCS have largely improved the accuracy and enlarged the application fields of traditional FCS technique. In this review, we will focus on both traditional and novel applications of FCS to investigate flow profiles and cellular biochemistry.

## Theory of FCS

Contrary to conventional single molecule set-ups, FCS does not rely on the intensity of emission, but instead on spontaneous fluctuations of fluorescence intensity caused by deviations from a mean. Autocorrelation is a measure of self-similarity of a time signal. In this case (Equation 1) a fluorescence signal at a certain time,  $F(t)$  is measured against the time-averaged signal over time  $\langle F(t) \rangle$ . The time-dependent fluctuation is calculated as

$$\delta F(t) = F(t) - \langle F(t) \rangle. \quad \text{Equation 1}$$

In many cases, autocorrelation is calculated from the time trajectories of a fluorescence signal. The intensity information is therefore preserved, and alongside FCS data can improve the information content of the measurement. When using a confocal set-up, the fluctuations from the temporal average give rise to an autocorrelation curve, which is defined as:

$$G(\tau) = \frac{\langle \delta F(t) \delta F(t+\tau) \rangle}{\langle F(t) \rangle^2}. \quad \text{Equation 2}$$

The resultant autocorrelation signal,  $G(\tau)$ , is calculated with respect to the self-similarity of the fluorophore diffusing in and out of the probe volume after lag time ( $\tau$ ) under laser irradiation. The autocorrelation curve can then be fitted with a mathematical model that gives quantitative information such as diffusion time ( $\tau_D$ ), number of molecules in the probe volume ( $\langle N \rangle$ ), diffusion coefficient ( $D$ ), or molecular brightness ( $\eta$ ). One of the advantages using FCS is that different models can be used to extract parameters that are specific to different applications. For example, in membrane measurements, the 2D Gaussian detection is defined by the intersection of the laser with the membrane. Giving rise to the 2D model

$$G(\tau) = \frac{1}{\langle N \rangle} \left( 1 + \frac{\tau}{\tau_D} \right)^{-1}, \quad \text{Equation 3}$$

where  $\langle N \rangle$  is the average number of particles in the detection area, and  $\tau_D$  is the diffusion dwell time. For measurements in solution, the probe volume is defined by a 3D Gaussian profile, in which a 3D Brownian diffusion model can be used,

$$G(\tau) = \frac{1}{\langle N \rangle} \left( 1 + \frac{\tau}{\tau_D} \right)^{-1} \left( 1 + \frac{\tau}{S^2 \tau_D} \right)^{-1/2}.$$

The 3D diffusion model not only incorporates terms from the 2D model (Equation 3), but also includes an  $S$  term, which defines the shape of the probe volume (the ratio of the  $z$  and  $xy$  radii,  $w_z/w_{xy}$ ). In order to confirm that the shape of the confocal volume does not change, alignment of the system should be verified daily with a dye with a known diffusion

coefficient. Lastly, FCS serves as a sensitive method to measure flow-based effects. In this model, since the autocorrelation is not only a result of diffusion, but also superimposed flow, an active transport model is used,

$$G(\tau) = \frac{1}{\langle N \rangle} \left(1 + \frac{\tau}{\tau_D}\right)^{-1} \left(1 + \frac{\tau}{S^2 \tau_D}\right)^{-1/2} e^{-\left(\frac{\tau}{\tau_F}\right)^2 \left(1 + \frac{\tau}{\tau_D}\right)}$$

In this case,  $\tau_F$  is the flow dwell time, and both flow and diffusion play a role in mass transport of the fluorophore. As mentioned earlier, FCS measures the fluctuations of a signal over time (Figure 1A). In a typical autocorrelation curve, (Figure 1B), the amplitude of the curve is equal to  $1/N$ , and the point of inflection gives rise to the diffusion time ( $\tau_D$ ) of the fluorescent molecule migrating in and out of the probe volume.

## Typical Confocal FCS System

In a typical FCS set-up, excitation occurs with a laser. In our lab, a 488 nm continuous wave Ar<sup>+</sup> laser is used, although diode lasers and frequency-doubled Nd:YAG lasers are also common. The attenuated laser beam is directed to the back of a high numerical aperture objective by a longpass dichroic mirror, and the same objective collects the fluorescence from the sample. A tube lens is used to focus the collected fluorescence emission to a pinhole at the conjugate image plane. The pinhole is essential to the confocal system in that it provides a small detection volume (usually ~ 1fL) due to the rejection of out-of-focus light. In two-photon excitation FCS, the pinhole can usually be omitted. Upon exiting the confocal pinhole, the fluorescence is directed to a detector. Typically, single-photon counting avalanche photodiodes (APDs) are used. The pulses from the APDs are relayed onto a counting board, and then to a hardware or software correlator. It is important to note that many hardware correlators do not allow the raw (time trajectory) data to be saved as well. Software correlators, using photon counting boards, offer more flexibility but may suffer at higher acquisition speeds relative to a dedicated, hardware correlator. Figure 2 shows a typical confocal FCS system, although there are many variations on this theme, depending on the investigator and the application at hand.

## Application of FCS in microfluidic measurement

To date, microfluidic systems have been widely used in chemical, biochemical and environmental areas based on the advantages of reduced sample consumption, short analysis time and high sensitivity. Therefore, the measurement of flow parameters in microstructures is important to these applications. However, due to the structure constraints, one of the barriers in microfluidic design and development is the difficulty to probe flow and mass transport in microsystem. Although beads can be used to trace flow, the beads themselves may affect flow in the microchannel, and therefore diffusion effects cannot easily be identified. FCS, however, can be applied to investigating the flow profiles and determining the flow rate, as well as analyzing the diffusion-based motion and measuring the diffusion coefficient in the absence of flow in the microsystem. No beads are needed in FCS and therefore one only needs to add an extremely low concentration (10 pM-10 nM, depending on the instrument sensitivity) of fluorescent molecules to measure the flow properties. As a nondestructive tool, FCS has overcome some barriers of previous approaches such as flow disturbances, bead-surface interactions, and insufficient resolution of the flow in miniature structures.<sup>5</sup> Another important benefit of FCS in microfluidics is the high spatial resolution that results from small measurement dimension. Mapping a flow profile can be achieved by scanning the probe volume in the microstructure.

Recently, several groups have reported the hydrodynamic investigations of monitoring flow using FCS in microchannels, -reactors and -mixers. Gösch *et al.* used standard FCS for mapping a two-dimensional parabolic flow profile in a  $50 \times 50 \mu\text{m}^2$  channel.<sup>5</sup> In Gösch's study, the primary parameter of interest was the flow time of molecules traversing the probe volume. By scanning the microchannel from top to bottom and from right to left with the laser focus, flow times of molecules were measured. Therefore, a map of the flow profile was obtained at different flow rates. FCS measurements of flow have been shown to be linear over a large range.<sup>32</sup>

FCS can not only be applied to determine flow profiles in straight channels, but also in channels with junctions. Our group has designed a low-shear chip for cell culture, in which the low-shear mass transport was generated at a T-shaped junction in the microchannel.<sup>33</sup> Fluorescence recovery after photobleaching was used to estimate the volumetric flow rate in the channels, but diffusion measurements could not be determined in the intersection of the two channels. To measure the flow velocities at the intersection accurately, FCS was used to map the flow profile in a microfluidic vortex.<sup>18</sup> Figure 3A shows the layout of the microchannel with T-shape junction from top view. The junction between main channel and side channel was divided into nine positions and flow velocities were measured separately at these nine spots. Different colors represented different flow velocities. Autocorrelation curves were obtained by autocorrelation function of 3D transport models. Larger  $\tau_D$  and  $\tau_F$  values indicate slower mass transport. Figure 3 shows flow in the center of the junction was slowest and the vortex-like flow generated at the intersection of T-shape junction. While flow preceding the T-shaped junction was determined to be laminar, flow in the junction exhibited a vortex-like flow. In this work, FCS played an important role to investigate the mass transport in the microstructure. The vortex-like flow was responsible for low-shear mass transport that enabled cell culture in the device. Therefore, flow profile determination via FCS is critical for biological studies as well as hydrodynamics.

In addition to microchannels, FCS can measure the flow velocities in other microstructures.<sup>6,34</sup> Visser's group followed the same procedure outlined by Gösch to study the flow in a microcapillary. Using FCS, it was observed that due to optical forces produced by the laser beam, the flow time of microspheres and bacteria in the capillary increased with increasing excitation power. However, for small molecules such as Rhodamine Green, the laser power did not affect the flow time in microcapillary.

FCS has also been used to determine the diffusion coefficient in microfluidic mixers.<sup>19,35</sup> Microfluidic mixers have been successfully applied to the investigation of protein and RNA folding<sup>36,37</sup> and Förster Resonance Energy Transfer (FRET).<sup>38,39</sup> In work by Park *et al.*, a five-inlet port mixer was designed to study macromolecular conformational change under various conditions.<sup>19</sup> FCS was used to characterize the jet flow speed along the axial center in the mixer when the flow was directed to the channel from five inlets at different flow rates. Liao *et al* combined zero-mode waveguides with FCS in a continuous flow microfluidic mixer. Comparing the signal to noise ratio of standard diffraction-limited FCS in rapid flow, it was demonstrated that zero-mode waveguides improved the signal to noise ratio and reduced the uncertainty in the kinetic analysis and diffusion coefficients determinations. In addition, advection effects of standard FCS can be eliminated via zero-mode waveguides in a diffusive mixer.<sup>35</sup>

FCS can be employed in many different fields, but it still has some limitations and artifacts such as inaccuracy and the lack of models. Recently some novel techniques that are extensions of FCS have overcome some weaknesses and improved the sensitivity and accuracy for flow measurements. Fluorescence cross-correlation spectroscopy (FCCS) eliminates many artifacts, in the application of flow measurement, such as insensitivity to

flow direction and phase fluctuation which may lead to complicating the experimental measurement.<sup>40–42</sup> When applied to flow investigations, FCCS systems have two detection regions created by two laser beams and the fluorescence emission from two regions is measured by separate detectors. The cross-correlation function introduces two coordinates for two volume elements and correlates the fluctuation from the first volume element, defined as  $\delta F_1(t)$ , and fluctuation from second volume element, defined as  $\delta F_2(t + \tau)$ , where  $\tau$  is the correlation time interval. The correlation curve will arrive at its maximum for the time the molecule moves from first focus to the other. By introducing a constant distance between the first and second focus the errors due to many hard-to-control parameters can be eliminated. In an early application of flow FCCS, researchers from Oklahoma state university and Chinese University of Hong Kong developed an incoherent technique featuring two-color cross-correlation to obtain local velocity by measuring particle transit time.<sup>40,41</sup> Other groups also reported improvement of the dual-focus FCCS technique used in flow profile investigation. Dittrich and co-workers compared one- and two-photon excitation in dual-beam FCCS, and it was observed that the probe volume in two-photon excitation system can be made smaller. In addition, two-photon excitation could suppress undesired cross-talk between the two detection volumes.<sup>43</sup> Researchers from the Russian Academy of Sciences investigated the flow near the hydrophilic and hydrophobic walls in microchannels using two-focus FCCS.<sup>44</sup> Recently, the Enderlein group introduced a modified method of dual-focus FCS (2f FCS) with overlapped confocal volumes and applied it to diffusion coefficient determination and velocity flow profiles.<sup>26,45</sup> 2fFCS was used to map the flow profile in a microcapillary. The measurement was performed using an inverted fluorescence microscope and two diode lasers, which produced two overlapped detection regions. It was demonstrated that by using pulsed interleaved excitation (PIE) in an alternating fashion, a pseudoautocorrelation, which distorted the measurement, can be avoided.

Figure 4A represents two confocal volumes and Figure 4B shows the parallel and orthogonal orientation indicated that velocity can be measured in either direction. The yellow and black curves in Figure 4B showed the autocorrelation from each focus via which the flow velocity can be estimated. The blue and red curves were from the forward and reverse cross-correlations, respectively, and flow directions were derived from these two curves. The cross-correlation curve reached its maximum for the time the molecule traversed from  $f_1$  to  $f_2$ . It was also observed that the peak of cross-correlation curve only occurred when the molecule moved forward, from first focus to second focus, but not in reverse movement. Therefore it was demonstrated that 2f FCS possessed the ability of accurate measurement of flow velocity and determination of flow direction in microstructures. In addition, by introducing an external ruler, which was a constant distance between two focal axes, the error from the value of laser beam waist radius ( $\omega_0$ ) in conventional FCS could be largely eliminated. Although 2f FCS is more accurate and useful in flow measurement, it is still not suited for near-wall region measurement in microfluidics.

Total Internal Reflection (TIR) illumination in conjugation with FCS has proven to be an effective method to study the liquid flow near a solid surface. Figure 5 shows the conceptual basis of the TIR-FCS system. Total Internal Reflection Microscopy (TIRM) is a powerful tool for the study of dynamical properties of liquid-solid interface due to the high axial resolution.<sup>46–48</sup> To date, TIR-FCS has been applied to diffusion and flow study in several groups.<sup>49–51</sup> Yordanov presented TIR-FCS as a novel method to determine the flow profile in the range of 0–200 nm from interface in microchannel.<sup>51</sup> In this work, the evanescent wave was created by an optical coupling system composed of a collimator and a prism reflecting element that coupled the light into the system. The incident angle at the channel wall can be adjusted by changing the tilt of the reflecting element in optical coupling system and therefore penetration depth could be varied in the range of 80–200 nm. The flow

velocity at different distances from the interface can be measured by adjusting the penetration depth. The effect of the size of the tracer molecules resulting from the interaction with the solid surface as well as ionic strength and distance between the probe volumes were also investigated in this work.

Another limitation for FCS in microfluidics is the lack of a suitable interpreting model under different conditions, especially when measurements are performed in microchannels where boundary effects can not be neglected. Therefore, some groups focused on the autocorrelation function models under non-standard conditions in order to obtain reliable results in microstructure. Formulations were proposed via Numerical FCS to predict the correlation functions by some researchers.<sup>52,53</sup> Recently, a closed form solution for FCS used for flow profiling in constrained conditions was introduced by Sanguigno.<sup>54</sup> The model, based on the assumption of elastic interactions at the walls, had the capability of acquiring reliable results in microstructures and was important to the study of mass transport process in microchannels.

## FCS in Biological Analyses

There has been a surge in the application of FCS in biological systems in the last ten years. As mentioned before, this is mostly due to the development of confocal single molecule microscopy using sensitive detectors. Improvements in detectors and optics have allowed lower excitation irradiances to be used, reducing phototoxicity and photobleaching. One of the reasons that FCS has been brought to the biological forefront is the work done by Schuille and coworkers. In their work in *Nature Methods*<sup>55</sup>, Schuille *et al.* provides a step-by-step protocol for labeling, detecting, and analyzing FCS in cells. In addition, the authors also provided protocol methods for dual-color fluorescence cross-correlation spectroscopy (FCCS)<sup>56</sup>, and two-photon methods for both FCS, and FCCS.<sup>57-58</sup> Due to these advancements, work has been done to elucidate membrane structure<sup>59</sup>, protease activity<sup>60</sup>, enzyme kinetics<sup>61</sup>, molecular transport<sup>62</sup>, and much more.

When using FCS to determine enzyme kinetics, the change in mass between enzyme and enzyme-substrate complexes is small. Because FCS is based on the molecular dynamics of diffusion on a logarithmic time scale, the changes of bound and unbound complexes can be unrecognizable. However, FCCS was developed to solve this drawback. In FCCS excitation is performed with two different lasers, and the fluorescence collected is divided into two different channels. The two signals (e.g. red and green) are measured simultaneously and cross-correlated. The result is that both species are labeled, and only the species that are bound are cross-correlated. Cross talk can be a problem when using dual color systems. Emission filters should be far apart, spectrally, in order to avoid transmission overlap. In addition, FCCS requires high spatial overlap; meaning, the two laser beams should have exact spatial superposition, so the focal volumes also overlap. Cross talk can be avoided by choosing fluorophores that have very different emission peaks. In work by Lee and coworkers, the authors developed a dual-color FCCS system that is capable of cross-talk-free analysis in near real time. The authors used two fluorophores, Cy3 and IRD800, which are spectrally distinct (difference in emission peaks ~250nm) and were excited simultaneously using two lasers, in order to prevent cross-excitation, cross-emission, and fluorescence energy transfer (FRET). Using their instrument, the authors demonstrate the ability to detect the enzyme activity of APE1, an enzyme that is responsible for cleaving the phosphodiester backbone in DNA. The authors observed no signal leakage from cross-talk or FRET, and confirmed the results through autocorrelation analysis of the fluorescence signals on each detection channel and autocorrelation analysis between the two color channels.<sup>24</sup>

FCCS has been developed to solve the drawbacks of FCS, especially in distinguishing two species with similar molecular weights. Although FCCS requires a high degree of spectral separation between fluorescently labeled molecules, and spectral overlap in order to prevent signal bleed through,<sup>56</sup> it is a very sensitive method. In addition, there are also different forms of FCS that have addressed drawbacks of FCCS. In work by Chen *et al.*, the authors overcome these major drawbacks in their demonstration of the ability of Fluorescence Lifetime Correlation Spectroscopy (FLCS) to study protein-receptor interactions in live cells.<sup>63</sup> FLCS combines FCS with time-correlated single photon counting (TCSPC). This allows the separation of autocorrelation based on different lifetimes and allows species with similar diffusion times to be distinguished.<sup>64</sup> FLCS has the advantages of requiring only one excitation source and is also immune to spectral cross-talk and signal bleed through.

FCS can also be used to measure surface receptor density in living cells (Figure 6).<sup>16</sup> While flow cytometry has been a standard method for measuring surface receptor density<sup>65</sup>, it cannot be used to measure receptor density for aptamers, or for cases when primary antibody calibration beads are not available. The number of receptor ligands is determined by the amplitude of the autocorrelation function. The ratio of bound and unbound receptor ligands is determined to calculate the number of membrane receptor molecules in the probe beam focus. If the beam radius is known, the surface density can be calculated. This method works with any cell surface marker that has a fluorescent probe, including markers such as lipids, which typically do not have antibodies readily available.

FCS has also been utilized in membrane structure elucidation. Understanding biological processes that occur at the membrane are essential. Most of the cells important reactions occur on the membrane, including, immune response, ion transfer, and receptor-ligand interactions. In work done by the Savatier group, the authors used two-photon, two-color, fluorescence cross correlation spectroscopy (FCCS) to measure the interactions of estrogen receptor (ER) subtypes  $\alpha$  and  $\beta$ , in transfected COS-7 cells, with transcriptional co-regulator protein, TIF2. In addition, the authors studied the heterodimerization of ER subtypes, and presented the first quantitative measurement of the full-length coactivator. The authors did so using a blue fluorescent protein, cerulean, fused to the N terminus, in addition the co-regulator was fused to the red mCherry fluorescent protein. Concentration and diffusion times were determined from autocorrelation curves, and showed significant differences in protein interaction affinities as a function of protein concentration.<sup>66</sup>

One of the novel techniques for cellular analysis is combining total internal reflection and FCS. This method provides a smaller probe volume than confocal instruments. FCS requires a small number of fluorescently labeled species in order to obtain effective correlation. This can be controlled in *in vitro* experiments, but it is not readily possible to control fluorescently labeled species in a cell. However, by using an evanescent wave to excite molecules, the observation volume can be reduced to attoliters ( $10^{-18}$ L).<sup>67</sup> This reduction in volume allows the effective excitation of single molecules within a cell. The method has been demonstrated by using TIR-FCS to measure fluctuations from fluorophores moving in and out of the evanescent wave.<sup>68</sup> The authors were able to obtain information about the diffusion coefficients of particles, and the depth of the evanescent wave. In addition, this method proved to be ideal for membrane measurements and was later used to measure the concentration and diffusion coefficients of fluorescently labeled IgG close to membranes (Figure 7).<sup>69</sup> Advanced applications of this technique include using cross-correlation TIR-FCS to measure dual-labeled, double-stranded DNA diffusing through the evanescent wave<sup>70</sup>, and using TIR-FCS to study lateral mobility in farnesylated enhanced green fluorescent protein (F-EGFP) in HeLa cells.<sup>71</sup> TIR-FCS is quickly becoming a useful and capable technique in the cellular analysis.



There is also application of using FCS with new types of probes. In work done by Hui *et. al.* fluorescent nanodiamonds, (FND) containing nitrogen-vacancy defect centers, were used as fluorescent probes.<sup>72</sup> The authors compared one-photon and two-photon confocal scanning fluorescence correlation spectroscopy in bare FND particles spin coated on glass slides, and also single FNDs in HeLa cells. The authors observed that the intensity ratio between the FND fluorescence and the autofluorescence from the HeLa cells by two-photon excitation is enhanced at least two times that of one-photon excitation. In addition, the authors conclude, that by combining two-photon FCS with one-photon single particle tracking (SPT), they were able to monitor both short-term, and long-term tracking of single FNDs in the complex environment of the cell.<sup>72</sup>

In work by Wells *et. al.*, the authors demonstrate the use of time-resolved 3D molecular tracking of individual quantum dot-labeled signaling molecules on and inside living cells. Trajectories were measured for minutes and were extended up to 10um in all spatial dimensions. This enabled the tracking of particles throughout the entire volume of the mammalian cells. In addition, the authors were able to utilize FCS to analyze the fluctuations of emission intensity during the trajectory, and demonstrate that FCS could be performed on a live cell for an extended amount of time as molecules are moving at biological rates.<sup>73</sup>

Recently, our group was able to utilize FCS in the detection of caspase activity.<sup>74</sup> We were able to rapidly identify apoptotic Jurkat cells by the cleavage of a sensitive probe of caspase-3 activity, bis(L-aspartic acid)-rhodamine 110 (D<sub>2</sub>R). Apoptosis was induced via the extrinsic pathway with anti-CD95 antibodies. Autocorrelation curves were generated as a result of the D<sub>2</sub>R being cleaved by activated caspases. The cleaved probe resulted in free rhodamine 110 diffusing in and out of the probe volume. Autocorrelation curves were drastically different between blank Jurkat cells, control cells, and cells that had activated caspases. This method was used to successfully distinguish apoptotic cells from autofluorescent (non-apoptotic) cells as early as 45 minutes after apoptosis induction. This method has proven to have several advantages over conventional techniques, including high temporal resolution and sensitivity. In addition, this method allowed the cells to be kept viable for further analysis, and did not require transfection of the cells.

## Conclusion

Fluorescence correlation spectroscopy and the extensions of this technique (FCCS etc.) have been demonstrated as useful techniques in research involving microfluidics and cellular analyses. Due to its high spatial and temporal resolution, short analysis times, and ability to lower sample consumption, it has quickly become a method to study chemical kinetics, molecular diffusion, concentration effects, and conformation dynamics. The goal of this Focal Point was to highlight two areas of study in which FCS has played a major role. In the realm of microfluidics and cellular analyses, several different parameters can be measured, which demonstrates an advantage of utilizing FCS based techniques.

FCS has matured since its introduction in the 1970s. It has become an information-rich technique, capable of nondestructive analysis that can complement other techniques. With the incorporation of FCCS, FLCS, TCSPC, and TIRFM-FCS the sensitivity, limits of detection, and overall figures of merit have improved. There will undoubtedly continued improvements in FCS methods, and the number of applications to which FCS has been applied will only continue to grow.

## Acknowledgments

The authors acknowledge support from the National Institutes of Health (grant RR025782) and the Robert A. Welch Foundation (Grant D-1667). M.M.M. was supported by a Provost's Fellowship from Texas Tech University.

## References

1. Magde D, Elson EL, Webb WW. *Phys. Rev. Lett.* 1972; 29:705.
2. Elson EL, Magde D. *Biopolymers.* 1974; 13:1.
3. Magde D, Elson E, Webb WW. *Biopolymers.* 1974; 4:29. [PubMed: 4818131]
4. Rigler R, Mets U, Widengren J, Kask P. *Eur Biophys J Biophys.* 1993; 22(3):169.
5. Gosch M, Blom H, Holm J, Heino T, Rigler R. *Anal Chem.* 2000; 72(14):3260. [PubMed: 10939397]
6. Kunst BH, Schots A, Visser AJWG. *Anal Chem.* 2002; 74(20):5350. [PubMed: 12403592]
7. Widengren J, Rigler R. *J. Fluoresc.* 1996; 7:211.
8. Magde D, Elson EL, Webb WW. *Biopolymers.* 1974; 13:29. [PubMed: 4818131]
9. Eigen M, Rigler R. *P Natl Acad Sci USA.* 1994; 91(13):5740.
10. Thompson, NL. *Topics in Fluorescence Spectroscopy.* Lakowicz, JR., editor. Vol. Vol.1. New York: Plenum Press; 1991. p. 337
11. Kinjo M, Rigler R. *Nucleic Acids Res.* 1995; 23(10):1795. [PubMed: 7784185]
12. Schwille P, Oehlschlager F, Walter NG. *Biochemistry-U.S.* 1996; 35(31):10182.
13. Schuler J, Frank J, Trier U, Schafer-Korting M, Saenger WA. *Biochemistry-U.S.* 1999; 38(26): 8402.
14. Wohland T, Friedrich K, Hovius R, Vogel H. *Biochemistry-U.S.* 1999; 38(27):8671.
15. Margeat E, Poujol N, Boulahtouf A, Chen Y, Muller JD, Gratton E, Cavailles V, Royer CA. *J Mol Biol.* 2001; 306(3):433. [PubMed: 11178903]
16. Chen Y, Munteanu AC, Huang YF, Phillips J, Zhu Z, Mavros M, Tan WH. *Chem-Eur J.* 2009; 15(21):5327.
17. De Santo I, Causa F, Netti PA. *Anal Chem.* 2010; 82(3):997. [PubMed: 20047288]
18. Liu K, Tian Y, Burrows SM, Reif RD, Pappas D. *Anal Chim Acta.* 2009; 651(1):85. [PubMed: 19733740]
19. Park HY, Qiu XY, Rhoades E, Korlach J, Kwok LW, Zipfel WR, Webb WW, Pollack L. *Anal Chem.* 2006; 78(13):4465. [PubMed: 16808455]
20. Enderlein J, Gregor I, Patra D, Fitter J. *Curr Pharm Biotechno.* 2004; 5(2):155.
21. Marrocco M. *Appl Optics.* 2004; 43(27):5251.
22. Nishimura G, Kinjo M. *Anal Chem.* 2004; 76(7):1963. [PubMed: 15053658]
23. Hac AE, Seeger HM, Fidorra M, Heimburg T. *Biophys J.* 2005; 88(1):317. [PubMed: 15501937]
24. Lee W, Lee YI, Lee J, Davis LM, Deininger P, Soper SA. *Anal Chem.* 2010; 82(4):1401. [PubMed: 20073480]
25. Culbertson MJ, Williams JTB, Cheng WWL, Stults DA, Wiebracht ER, Kasianowicz JJ, Burden DL. *Anal Chem.* 2007; 79(11):4031. [PubMed: 17447726]
26. Arbour TJ, Enderlein J. *Lab Chip.* 2010; 10(10):1286. [PubMed: 20445882]
27. Xiao Y, Buschmann V, Weston KD. *Anal Chem.* 2005; 77(1):36. [PubMed: 15623276]
28. Ruan QQ, Cheng MA, Levi M, Gratton E, Mantulin WW. *Biophys J.* 2004; 87(2):1260. [PubMed: 15298928]
29. Gielen E, Smisdom N, De Clercq B, Vandeven M, Gijsbers R, Debyser Z, Rigo JM, Hofkens J, Engelborghs Y, Ameloot M. *J Fluoresc.* 2008; 18(5):813. [PubMed: 18204890]
30. Kapusta P, Wahl M, Benda A, Hof M, Enderlein J. *J Fluoresc.* 2007; 17(1):43. [PubMed: 17171439]
31. Wennmalm S, Thyberg P, Xu L, Widengren J. *Anal Chem.* 2009; 81(22):9209. [PubMed: 19860428]

32. Brister PC, Kuricheti KK, Buschmann V, Weston KD. *Lab Chip*. 2005; 5(7):785. [PubMed: 15970973]
33. Liu K, Pitchimani R, Dang D, Bayer K, Harrington T, Pappas D. *Langmuir*. 2008; 24(11):5955. [PubMed: 18471001]
34. Ball DA, Shen GQ, Davis LM. *Appl Optics*. 2007; 46(7):1157.
35. Liao D, Galajda P, Riehn R, Ilic R, Puchalla JL, Yu HG, Craighead HG, Austin RH. *Opt Express*. 2008; 16(14):10077. [PubMed: 18607415]
36. Pollack L, Tate MW, Finnefrock AC, Kalidas C, Trotter S, Darnton NC, Lurio L, Austin RH, Batt CA, Gruner SM, Mochrie SGJ. *Phys Rev Lett*. 2001; 86(21):4962. [PubMed: 11384392]
37. Russell R, Millett IS, Tate MW, Kwok LW, Nakatani B, Gruner SM, Mochrie SGJ, Pande V, Doniach S, Herschlag D, Pollack L. *P Natl Acad Sci USA*. 2002; 99(7):4266.
38. Dittrich PS, Muller B, Schwille P. *Phys Chem Chem Phys*. 2004; 6(18):4416.
39. Michalet X, Jaeger M, Hertzog DE, Santiago J, Bakajin O, Weiss S. *Biophys J*. 2005; 88(1):33a.
40. Tong P, Xia KQ, Ackerson BJ. *J Chem Phys*. 1993; 98(12):9256.
41. Xia KQ, Xin YB, Tong P. *J Opt Soc Am A*. 1995; 12(7):1571.
42. Schwille P, MeyerAlmes FJ, Rigler R. *Biophys J*. 1997; 72(4):1878. [PubMed: 9083691]
43. Dittrich PS, Schwille P. *Anal Chem*. 2002; 74(17):4472. [PubMed: 12236358]
44. Vinogradova OI, Koynov K, Best A, Feuillebois F. *Phys Rev Lett*. 2009; 102:11.
45. Dertinger T, Pacheco V, von der Hocht I, Hartmann R, Gregor I, Enderlein J. *Chemphyschem*. 2007; 8(3):433. [PubMed: 17269116]
46. Axelrod D, Burghardt TP, Thompson NL. *Annu Rev Biophys Bio*. 1984; 13:247.
47. Huang P, Guasto JS, Breuer KS. *J Fluid Mech*. 2006; 566:447.
48. Bouzigues CI, Tabeling P, Bocquet L. *Phys Rev Lett*. 2008; 101:11.
49. Hassler K, Leutenegger M, Rigler P, Rao R, Rigler R, Gosch M, Lasser T. *Opt Express*. 2005; 13(19):7415. [PubMed: 19498766]
50. Ries J, Petrov EP, Schwille P. *Biophys J*. 2008; 95(1):390. [PubMed: 18339763]
51. Yordanov S, Best A, Butt HJ, Koynov K. *Opt Express*. 2009; 17(23):21149. [PubMed: 19997354]
52. Gennerich A, Schild D. *Biophys J*. 2000; 79(6):3294. [PubMed: 11106632]
53. Milon S, Hovius R, Vogel H, Wohland T. *Chem Phys*. 2003; 288(2–3):171.
54. Sanguigno L, De Santo I, Causa F, Netti P. *Anal Chem*. 2010; 82(23):9663. [PubMed: 21038906]
55. Kim SA, Heinze KG, Schwille P. *Nature Methods*. 2007; 4:11.
56. Bacia K, Schwille P. *Nature Protocols*. 2007; 2:11.
57. Mutze J, Petraseck Z, Schwille P. *Journal of Fluorescence*. 2007; 17:6.
58. Kim SA, Heinze KG, Waxham MN, Schwille P. *Biophysical Journal*. 2005; 88:6.
59. Chiantia S, Ries J, Schwille P. *Biochemica et Biophysica Acta-Biomembranes*. 2009; 1788:1.
60. Kohl T, Hausteine E, Schwille P. *Biophysical Journal*. 2005; 89:4.
61. Heinze KG, Rarbach M, Jahnz M, Schwille P. *Biophysical Journal*. 2002; 83:3.
62. Dittrich PS, Schwille P. *Anal Chem*. 2002; 74:17. [PubMed: 11795786]
63. Chen J, Irudayaraj J. *Anal. Chem*. 2010; 82:15.
64. Woodburn JR. *Pharmacol Ther*. 1999; 82:241–250. [PubMed: 10454201]
65. Pappas, D. *Practical Cell Analysis*. New York: John Wiley & Sons; 2010.
66. Savatier J, Jalaguier S, Ferguson ML, Cavailles V, Royer CA. *Biochemistry*. 2010; 49:4.
67. Blom H, Kastrup L, Eggeling C. *Pharm. Biotechnol*. 2006; 7:51–66.
68. Leutenegger M, Lasser T. *Opt. Exp*. 2006; 16
69. Starr TE, Thompson NL. *J. Phys. Chem*. 2002; 106
70. Leutenegger M, Blom H, Widengren J, Eggeling C, Gosch M, Leitgeb RA, Lasser T. *J. Biomed. Opt*. 2006; 11
71. Oshugi Y, Saito K, Tamura M, Kinjo M. *Biophys J*. 2006; 91
72. Hui YY, Zhang B, Chang Y, Chang C, Chang H, Hsu J, Chang K, Chang F. *Opt. Exp*. 2010; 18:6.

73. Wells NP, Lessard GA, Goodwin PM, Phipps ME, Cutler PJ, Lidke DS, Wilson BS, Werner JH. Nano Letters. 2010; 10
74. Martinez MM, Reif RD, Pappas D. Anal. Bioanal. Chem. 2010; 396

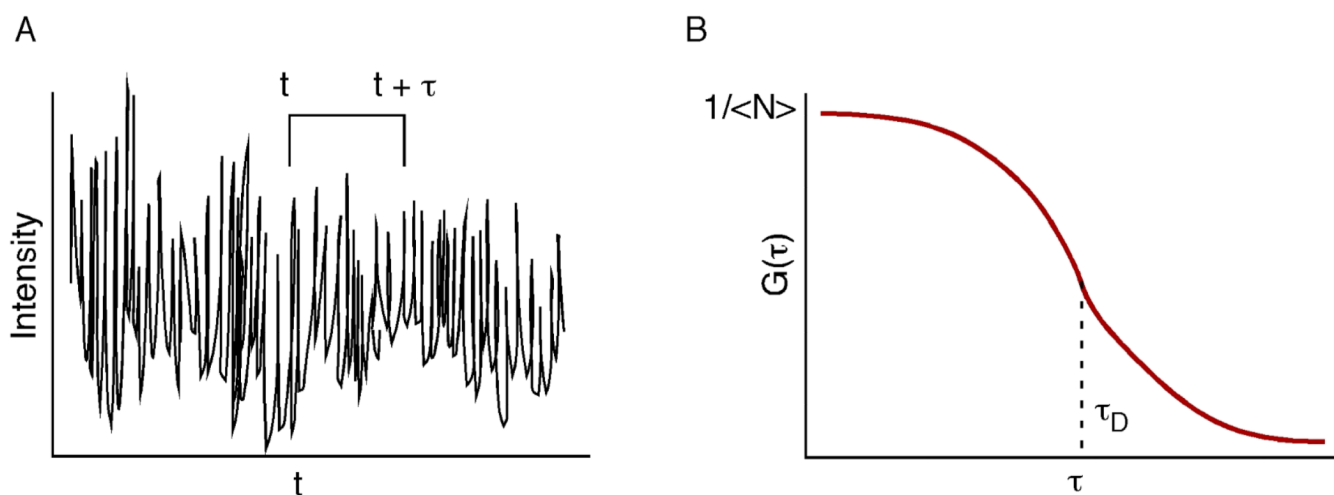


**Figure 1.** Conceptual diagram of a fluctuating fluorescence signal (A) as a function of time. The fluctuation of the signal is used to calculate the autocorrelation,  $G(\tau)$ , where  $\tau$  is the lag time from the original signal. The amplitude of the autocorrelation function (typically  $G(0)$ ) is inversely proportional to the average number of molecules in the probe volume ( $\langle N \rangle$ ).

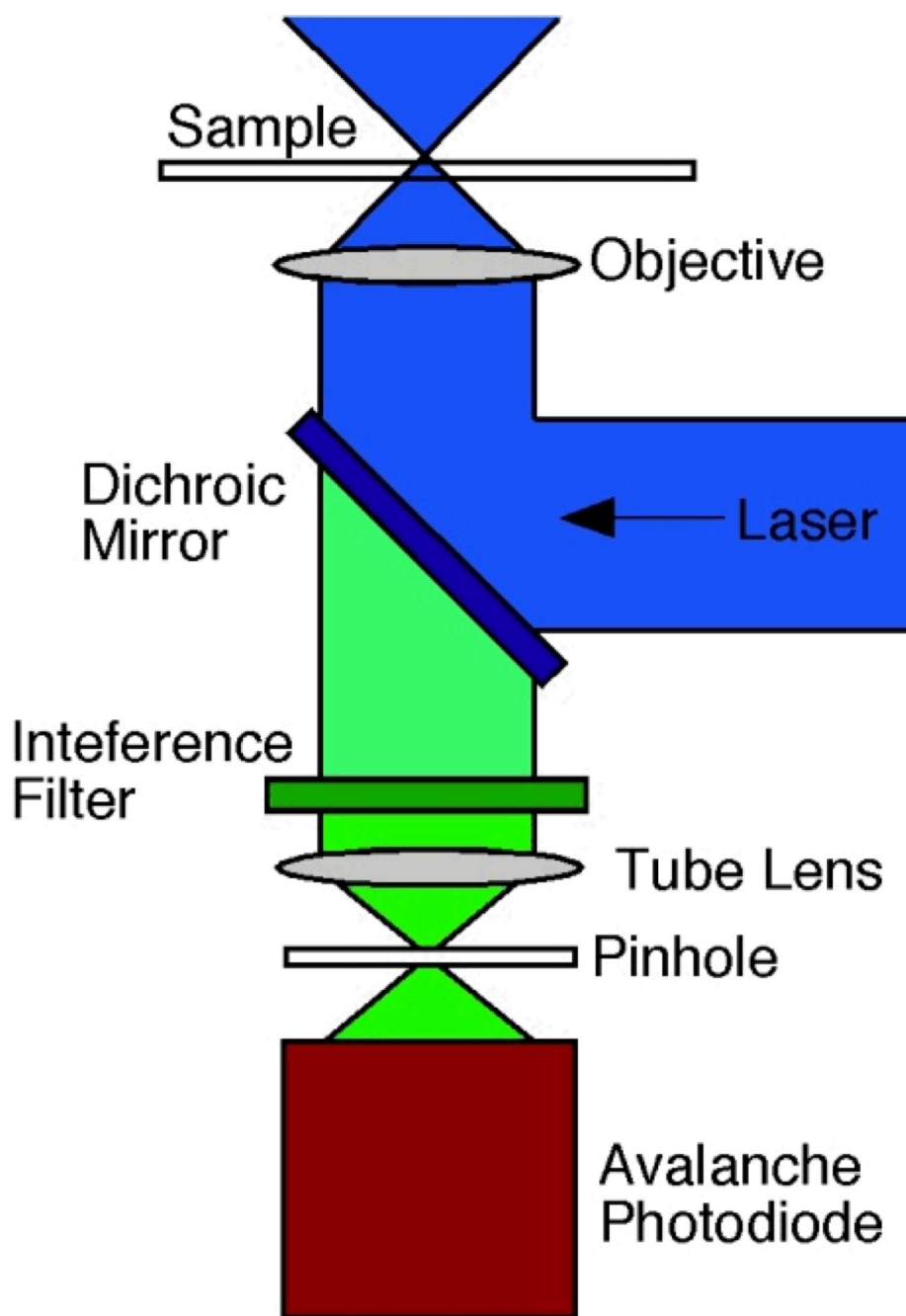


**Figure 2.**

A typical confocal FCS system. Laser light is focused by an objective (usually with high numerical aperture) to a diffraction limited spot. Fluorescence is collected by the same objective and filtered by an interference filter. A pinhole placed in the conjugate image plane reduces out of focus light. The pinhole is usually omitted in two-photon excitation

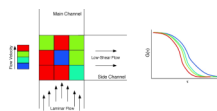


**Figure 3.** FCS measurements of flow in a low-shear cell culture chip. Laminar flow is disrupted at a T-channel interface, and FCS was used to probe the flow velocity in the junction. Flow was slowest in the center of the junction, indicating a vortex-like flow. Adapted from Reference 18.



**Figure 4.**

(A) Graphic visualization of the 2fFCS confocal volume and the nomenclature we use to describe its orientation relative to the direction of flow. (B) Typical fitted 2fFCS correlation curves. The four curves are comprised of two autocorrelations (one from each focus) and the forward and reverse cross-correlations. The data shown are for flow measurement in the “parallel” orientation, and therefore show a maximum in the “forward” cross-correlation. Adapted from Reference <sup>45</sup>.



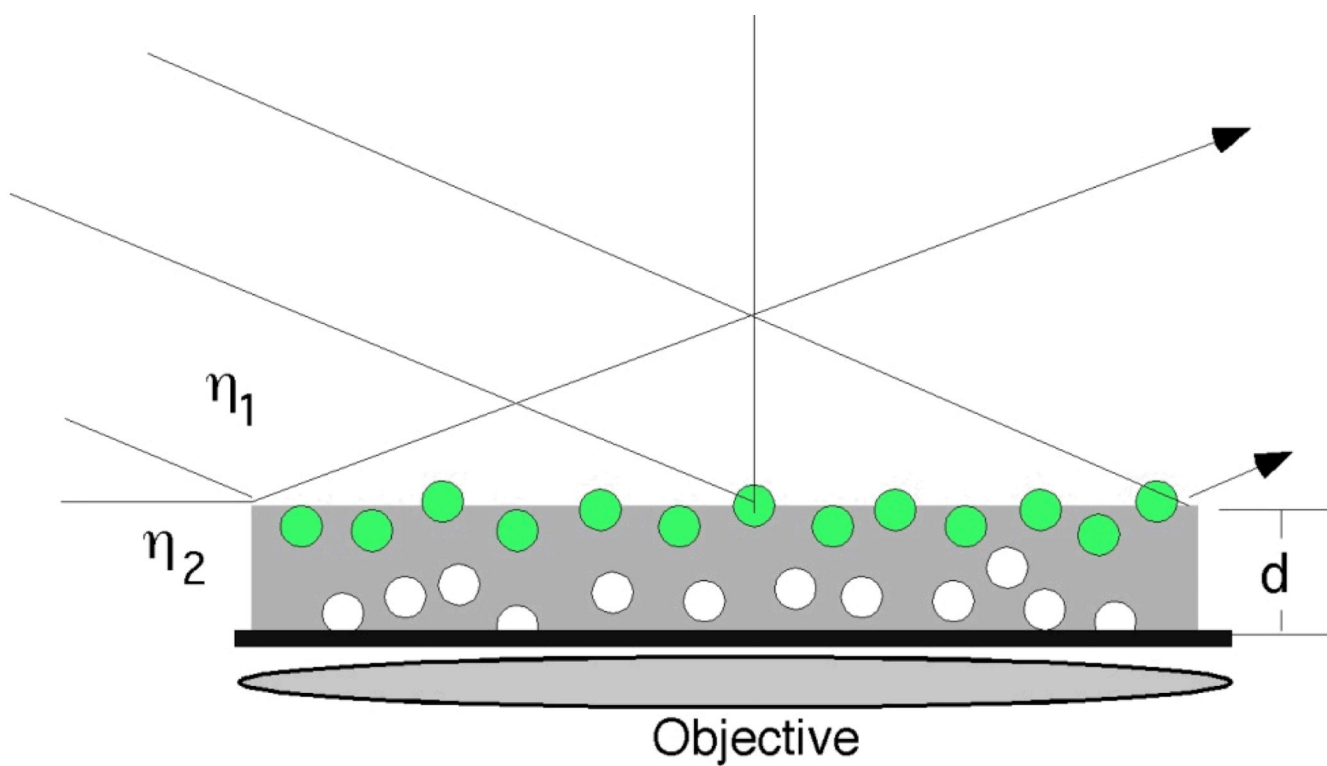


**Figure 5.** TIR-FCS. An evanescent wave generated using a prism or waveguide the top surface of the sample. A confocal microscope collects fluorescence from one spot, allowing signal to be restricted to close to the surface where total internal reflection of occurring. Adapted from Reference <sup>51</sup>.

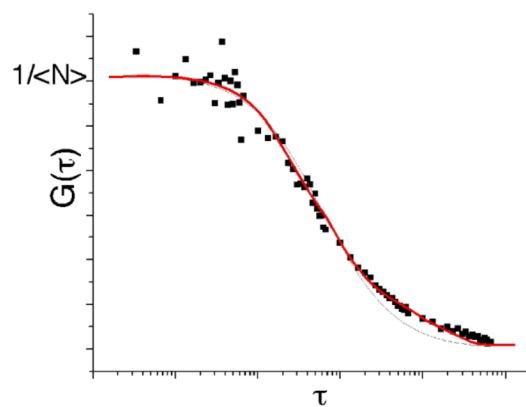
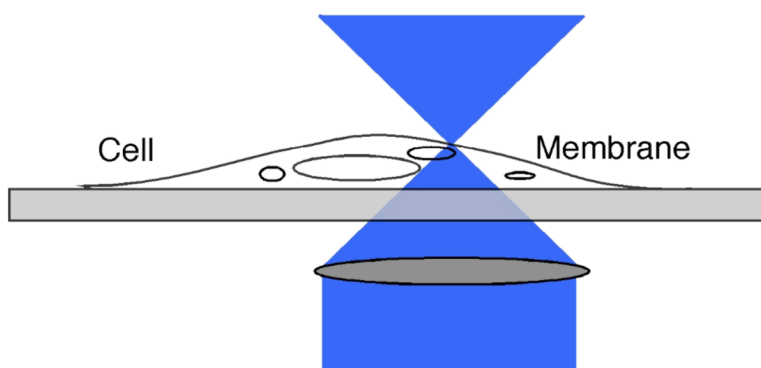


**Figure 6.** FCS measurements of surface receptor density. By focusing the laser spot of the cell membrane, the number of fluorophores in the probe volume (i.e. the membrane surface) can be estimated. The ratio of bound and unbound receptor ligands is also determined to calculate the surface density of any receptor using any fluorescent probe. Adapted from Reference <sup>16</sup> and 64.

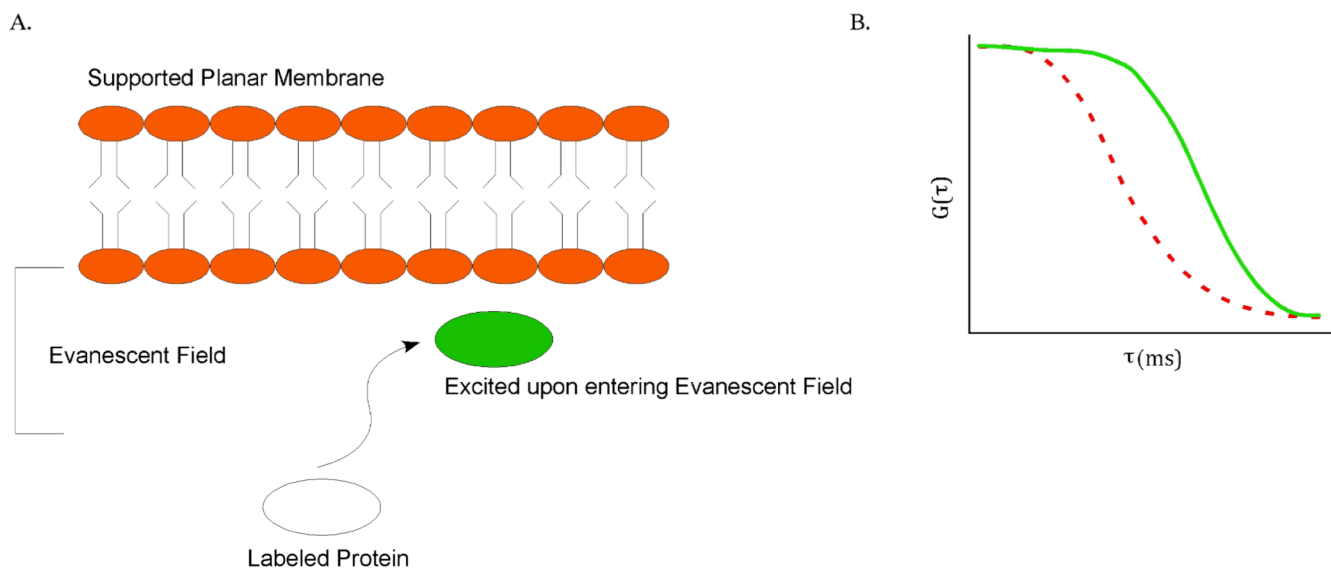


**Figure 7.** Schematic of soluble ligand binding on a planar membrane (a).  $K_a$  and  $K_d$  (association and dissociation rate constants) were later determined for IgG interacting with the planar membrane. The correlation curve on right (b) shows the TIR-FCS data of the diffusion of labeled IgG with unlabeled IgG close to the planar membrane (dotted red FCS curve shows small molecule diffusion in solution for comparison). Adapted from Reference <sup>68</sup>.